Cortexillins, Major Determinants of Cell Shape and Size, Are Actin-Bundling Proteins with a Parallel Coiled-Coil Tail

Jan Faix,* Michel Steinmetz,† Heike Boves,* Richard A. Kammerer,† Friedrich Lottspeich,* Ursula Mintert,* John Murphy,* Alexander Stock,* Ueli Aebi,† and Günther Gerisch*
*Max-Planck-Institut für Biochemie
D-82152 Martinsried
Federal Republic of Germany
†Biozentrum der Universität Basel
Klingelbergstrasse 70
CH-4056 Basel
Switzerland

Summary

Cortexillins I and II of D. discoideum constitute a novel subfamily of proteins with actin-binding sites of the α-actinin/spectrin type. The C-terminal halves of these dimeric proteins contain a heptad repeat domain by which the two subunits are joined to form a two-stranded, parallel coiled coil, giving rise to a 19 nm tail. The N-terminal domains that encompass a consensus actin-binding sequence are folded into globular heads. Cortexillin-linked actin filaments form preferentially anti-parallel bundles that associate into meshworks. Both cortexillins are enriched in the cortex of locomoting cells, primarily at the anterior and posterior ends. Elimination of the two isoforms by gene disruption gives rise to large, flattened cells with rugged boundaries, portions of which are often connected by thin cytoplasmic bridges. The double-mutant cells are multinucleate owing to a severe impairment of cytokinesis.

Introduction

Motile eukaryotic cells contain an impressive variety of proteins that modulate the organization and function of the actin–myosin system (Pollard and Cooper, 1986; Luna and Condeelis, 1990; Schleicher and Noegel, 1992). Proteins that directly bind to actin can be classified according to the structure of their actin-binding domains. α-Actinin, spectrin, dystrophin, filamin, and fimbrin are members of a superfamily characterized by a consensus sequence of about 226 amino acid residues that comprise their actin-binding domains. Proteins of this superfamily are typically cross-linkers of actin filaments. Most of them are anti-parallel homodimers or heterotetramers with actin-binding sites at each end (Hartwig and Kwiatkowski, 1991; Matsudaira, 1991). The rod domains of these proteins are formed by repeats of either triple α-helical or cross-β secondary structure (Hartwig and Kwiatkowski, 1991; Matsudaira, 1991).

Here we describe two proteins that are distinguished from the known members of the α-actinin/spectrin superfamily by the presence of a two-stranded coiled-coil tail domain, by which two subunits are assembled in a parallel, unstaggered fashion. By this arrangement, the actin-binding sites of the subunits are brought in juxtaposition, enabling them to cross-link actin filaments together into bundles. We have named these proteins cortexillins, because in the highly motile Dictyostelium cells they are preferentially located in the cortical region where actin filaments form high order structures of various shapes. Dictyostelium discoideum contains two cortexillins that are required for the cells to maintain their shape and undergo regular cytokinesis.

Results

Sequence Relationships of Cortexillin Isoforms

In a search of novel actin-binding proteins in D. discoideum, we precipitated actin–myosin complexes in a stepwise fashion from cell extracts and analyzed the associated proteins. One precipitate contained actin, myosin II, the known actin-binding proteins α-actinin and ABP-120, and an unidentified protein recognized as a 50 kDa polypeptide after SDS–polyacrylamide gel electrophoresis (SDS–PAGE). Partial amino acid sequence analysis suggested that this protein is a member of the α-actinin/spectrin superfamily of F-actin-binding proteins. Degenerated oligonucleotides were used to amplify a genomic 0.6 kb fragment by polymerase chain reaction (PCR). By probing a cDNA library with this fragment, we obtained a clone comprising the entire coding region. This clone encoded a polypeptide of 444 amino acids with a calculated molecular mass of 50.5 kDa. We designate this protein as cortexillin I.

The 0.6 kb genomic fragment hybridized to the 5′ portion of the cortexillin I coding region. Southern blots probed with this fragment under low stringency conditions indicated the presence of a related gene (Figure 1A, left). Probing the same blot with a 3′ cDNA fragment under high stringency revealed substantial differences between the two putative coding sequences in their 3′ regions (Figure 1A, right). These differences were exploited in searching for a cDNA clone that encodes the second protein. cDNA clones that hybridized with the 5′ fragment under low stringency were rescreened with the 3′ fragment under high stringency. One of the clones that did not hybridize with this fragment contained a complete coding region related to, but not identical with, that of cortexillin I. The encoded protein comprised 441 amino acids and had a molecular mass of 50.5 kDa. This protein will be referred to as cortexillin II.

Comparison of the cDNA-derived cortexillin I and II sequences revealed 60% identical residues over the entire sequences and 73% identity in their N-terminal halves (Figure 1B). The N-terminal halves of cortexillins I and II were clearly related to human α-actinin and β-spectrin, as shown for cortexillin I in Figures 1C and 1D. The less conserved C-terminal halves of cortexillins I and II proved to be most closely related to 23 different tail sequences of myosins in the database, in particular of myosin from Entamoeba histolytica (Raymond-Denise et al., 1993) and of muscle myosin II from Drosophila melanogaster (George et al., 1989), with a

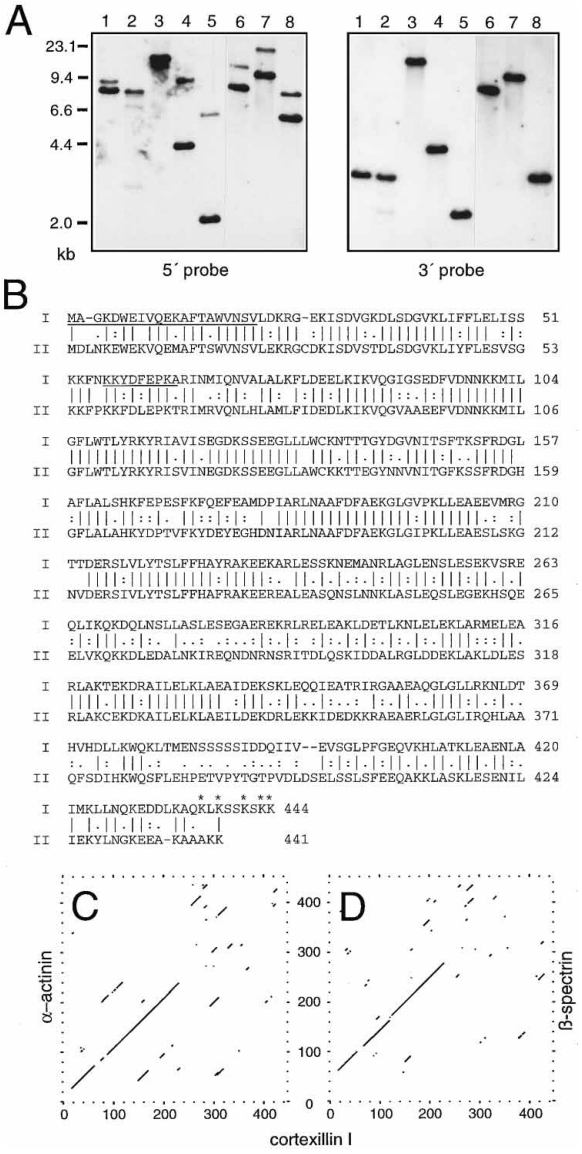

Figure 1. Cloning and Sequence Analysis of Cortexillins I and II

(A) Southern blot probed with cortexillin I DNA fragments showing the presence of two related genes. Left, a blot probed with a 5′ genomic DNA fragment under low stringency (30% formamide). Right, the same blot reprobed with a 3′ cDNA fragment under high stringency (50% formamide). In each digest only one fragment is labeled in the right panel and mostly two fragments are labeled in the left panel, indicating the presence of a gene cross-hybridizing with cortexillin I DNA in its 5′ region. Restriction enzymes used for lanes 1–8 are as follows: EcoRI (lane 1), EcoRI–HindIII (lane 2), HindIII (lane 3), XbaI (lane 4), XbaI–EcoRI (lane 5), SacI–HindIII (lane 6), BglII (lane 7), and BglII–EcoRI (lane 8).

(B) cDNA-derived amino acid sequences of cortexillins I and II. Portions confirmed by sequencing of intact cortexillin I or LysC peptides are underlined. Identical residues are connected by lines and similar residues by double and single dots according to the University of Wisconsin Genetics Computer Group BESTFIT program. Basic residues in the C-terminal nonapeptide sequence are indicated by asterisks.

(C and D) Dot blots showing sequence relationships of cortexillin I in its N-terminal half to the actin-binding domains of human nonmuscle α-actinin (C) and human β-spectrin (D). Similar relationships are valid for cortexillin II (data not shown). The sequences were compared using programs COMPARE and DOTPLOT (University of Wisconsin Genetics Computer Group) with window size 30 and stringency 15. Numbers on the Y axes refer to residues of α-actinin (Youssoufian et al., 1990) and β-spectrin (Hu et al., 1992), respectively; those on the X axis refer to residues of cortexillin I (including the methionine at the start site).

sequence identity on the order of 31% and a similarity of 53%. The cortexillin sequences show the highest overall relationship to a putative actin-binding protein deduced from a cDNA sequence of Physarum polycephalum (St-Pierre et al., 1993). The last nine residues of cortexillin I constitute a positively charged site resembling the putative phosphatidylinositol (4,5)bisphosphate (PIP_2) recognition site of other actin-binding proteins (Janmey et al., 1992; Hofmann, 1994). This cluster of positively charged amino acid residues is missing in cortexillin II.

Cortexillins I and II Accumulate in the Cortical Region of Dictyostelium Cells

Cortexillins I and II were purified as His-tagged proteins from Escherichia coli and injected into mice to raise monoclonal antibodies (MAbs). Antibodies that specifically recognized either cortexillin I or II were employed for immunofluorescence labeling of cells in the growth phase and aggregation stage (Figure 2A). The antibodies showed cortexillins to be localized to the cytoplasmic space; nuclei appeared as dark areas. Both cortexillins were enriched in regions of the cell cortex, including leading edges and crown-shaped extensions at the upper surface of growth-phase cells (Figures 2B and 2C). In the elongated cells of the aggregation stage, the cortexillins were enriched in the anterior region and, to a minor extent, at their posterior end (Figures 2D and 2E).

Cortexillin I Is a Parallel Dimer with Two N-Terminal Heads and a Coiled-Coil Tail

To study the molecular architecture of cortexillin I, a His-tagged recombinant protein was purified from E. coli lysates and analyzed by circular dichroism (CD) measurements, analytical ultracentrifugation, and electron microscopy. The CD spectrum had minima at 208 and 222 nm, characteristic of α-helical structures, the content of which was calculated to be 60%–70%.

The S value of the recombinant cortexillin I was determined from sedimentation velocity and its molecular mass (M_r) from sedimentation equilibrium. Sedimentation velocity at 56,000 rpm in 150 mM NaCl revealed an S value of 4.0, considerably larger than that of a globular protein of 50 kDa. A single sharp boundary was observed, indicating that the sample was homogeneous. Sedimentation equilibrium measurements at 12,000 rpm yielded a M_r value of 102 kDa. These values are consistent with cortexillin I being an elongated dimeric molecule.

Cortexillin I molecules were imaged by transmission electron microscopy (TEM). As the low magnification overview in Figure 3A (top) and the gallery (bottom) show, the cortexillin I dimers consist of two globular heads of 4–6 nm diameter attached in a flexible manner to a straight tail. For the rods, as displayed in the top row of the gallery in Figure 3A, a mean length of 19.3 nm with a standard deviation of ±1.0 nm was calculated

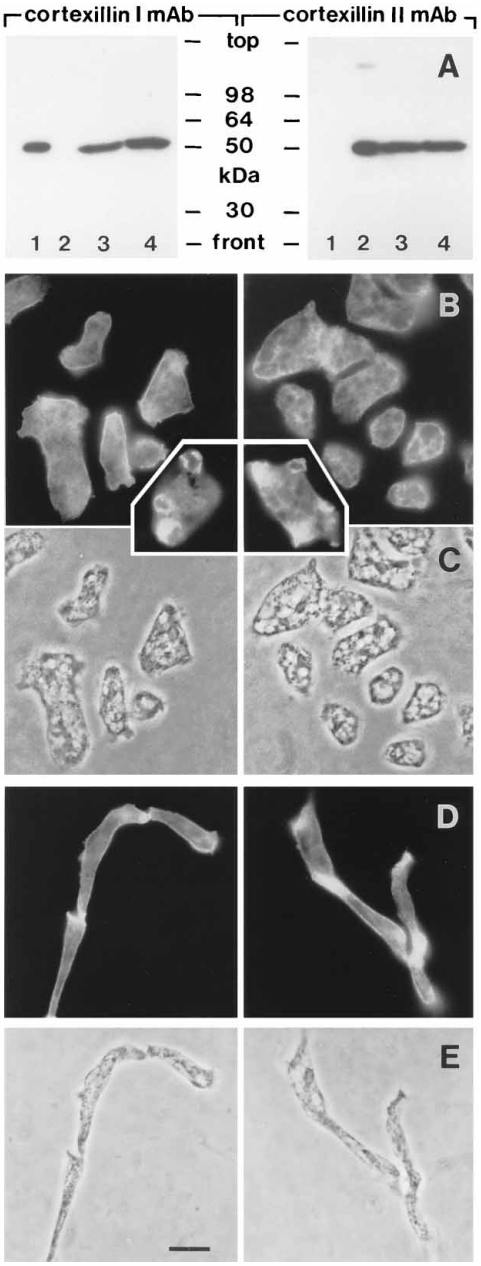

Figure 2. Immunofluorescence Labeling of Growth-Phase and Aggregating Cells of D. discoideum with Antibodies Specific for either Cortexillin I or Cortexillin II

(A) Specificity of the antibodies demonstrated in immunoblots of proteins from E. coli cells expressing recombinant His-tagged cortexillins I or II (lanes 1 and 2) or total proteins from growth-phase cells (lanes 3) or aggregation-competent cells (lanes 4) of D. discoideum. (B and C) Immunofluorescence and corresponding phase-contrast images of growth-phase cells. For the insets in (B), the focus was on the upper cell surfaces to show labeled crown-shaped extensions. (D and E) Immunofluorescence and phase-contrast images of aggregating cells. Cells in the left panel were labeled with cortexillin I–specific MAb 241-36-2 and those in the right panel with cortexillin II–specific MAb 232-238-10. Bar is 10 μm.

by fitting a Gaussian curve to the histogram of lengths (Figure 3C). About 30% of the cortexillin I molecules revealed a small, globular domain of 2–3 nm diameter at their tail region opposite to the two heads (bottom row of the gallery in Figure 3A). The mean length of these tails, including the globular end domain, was 22.6 nm with a standard deviation of ±1.0 nm (Figure 3D).

To localize the N-terminus of cortexillin I, we performed immunoelectron microscopy using MAb 232-470-5, an immunoglobulin G (IgG) that recognizes the N-terminal His tag sequence in the recombinant protein. As the overview of Figure 3B (top) and the gallery of selected cortexillin I antibody complexes (bottom) show, the antibody specifically labeled the globular heads of the cortexillin I molecule, thus demonstrating that the N-termini of the subunits reside in these heads.

In Figure 3E, the cortexillin I shape visualized by TEM was compared with structure predictions provided by the COILS algorithm of Lupas et al. (1991), which relates the sequence of a protein to sequences of known two-stranded coiled coils in a database. No tendency to assume a coiled-coil conformation was predicted for the N-terminal region of the cortexillin I sequence up to His-226. This region closely coincides with the sequence highly homologous to the actin-binding domains of α-actinin and spectrin (Figures 1C and 1D), which is proposed to fold into the globular heads of cortexillin I molecules.

Two sequence stretches were predicted to form α-helical coiled coils, one between Ala-227 and Arg-352 and the other between Phe-403 and Lys-438 (Figure 3E). For the first stretch, a high coiled coil probability of 0.99 was calculated. This stretch contains 18 continuous heptad repeats typical of α-helical coiled coils (Figure 3F). The theoretical length of 19 nm for a two-stranded α-helical coiled-coil domain comprising 18 repeats is in agreement with the average length measured for the cortexillin I rod domain (Figure 3C).

Cortexillin I Binds to F-Actin and Links the Filaments into Bundles and Networks

High speed centrifugation of F-actin with His-tagged cortexillin I indicated a pH optimum for binding between 6.0 and 7.0 (Figure 4A). The binding was Ca^{2+} independent (Figure 4B), in accord with the absence of a canonical Ca^{2+}-binding site from the sequence. The stoichiometry of about 1 cortexillin I dimer bound per 3–4 actin subunits indicates that cortexillin I molecules bind along the length of actin filaments (Figure 4C). From the binding data obtained at low cortexillin I concentrations, an approximate K_D on the order of 2.3×10^{-7}M is calculated, assuming that the two sites of a dimeric cortexillin I molecule bind independently to actin.

F-actin-cross-linking activity of cortexillin I was examined using low speed centrifugation and low shear viscometry. Most of the F-actin was pelleted at a ratio of 1 cortexillin I dimer to 10 actin subunits (Figure 4D). A strong gelatinizing activity was found using the falling-ball method for low shear viscometry (Figure 4E). At 1.1 μM cortexillin I, corresponding to one actin-binding site per five actin subunits, the steel ball became lodged in the gel.

TEM of negatively stained specimens revealed that cortexillin I causes dispersed, phalloidin-stabilized actin filaments to associate into bundles (Figures 5A and 5B).

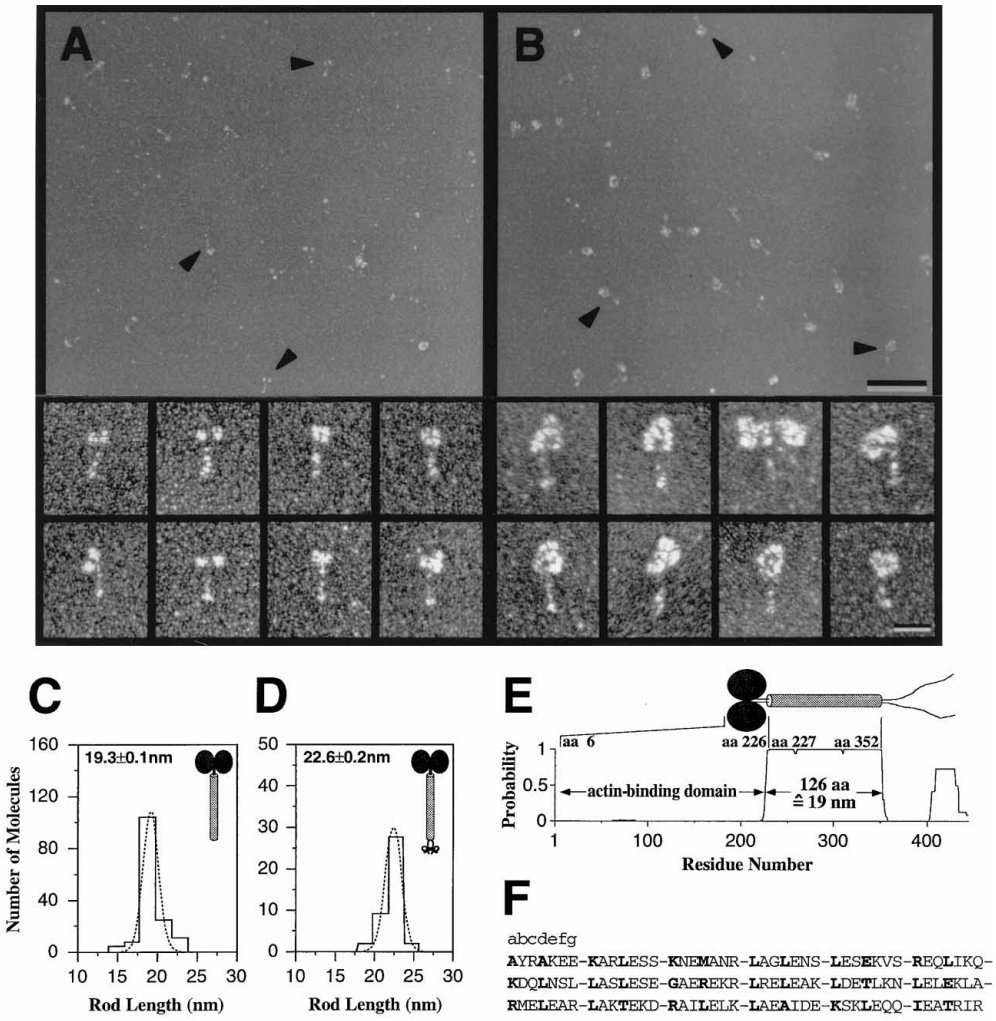

Figure 3. Electron Microscopic Analysis and Predicted Structure of Cortexillin I Molecules

(A) Recombinant cortexillin I molecules.

(B) Complexes of cortexillin I with MAb 232-470-5, which recognizes the His tag region added to the N-terminus of the protein. (A) and (B) show overviews on top (bar is 100 nm) and high magnification galleries at the bottom (bar is 20 nm). Specimens were prepared by glycerol spraying/low angle rotary metal shadowing.

(C and D) Distributions of molecular lengths of two types of cortexillin I rods that are distinguishable in the gallery of (A) (compare top with bottom panel). For (C), the lengths of 150 rods, and for (D) the lengths of 41 rods, were measured and displayed with single Gaussian fits. Insets show diagrams of the molecules measured in the corresponding panel; values are means ± standard errors.

(E) Head and tail domain of cortexillin I aligned to its amino acid sequence. The diagram shows the protein as a parallel dimer, based on the electron micrographs displayed in (A) and (B). The probability of forming parallel α-helical coiled-coil structures approximates the value of 1 throughout the sequence from Ala-227 to Arg-352. The sequence from Trp-6 to His-226 constitutes the consensus actin-binding domain, as shown in Figures 1C and 1D.

(F) The amino acid sequence from Ala-227 to Arg-352, which is predicted to form an α-helical coiled coil consisting of 18 heptad repeats. Positions in these repeats are labeled a through g.

These bundles were often interconnected, thus forming meshworks, in accord with the gelatinizing activity of cortexillin I. At a molar ratio of 1 cortexillin dimer to 11 actin subunits, the predominant structures were isolated bundles and single-layered arrays of actin filaments. In the arrays, fuzzy transverse bands were discernible with a spacing of about 36 nm (Figure 5C, arrowheads in the left panel), corresponding to one crossover spacing of the actin double helix.

Parallel or anti-parallel orientation of actin filaments in the bundles was assessed by determining the vorticity, i.e., the handedness, of individual filaments from axial projections of their three-dimensional reconstructions (Figure 5C, right). Of 21 processed pairs of filaments, 18 revealed opposite polarities of the adjacent filaments, and the other 3 displayed the same polarity.

Cortexillins Stabilize Cell Shape and Support Cytokinesis

To study the function of cortexillins in vivo, we eliminated cortexillins I and II, together or individually, by gene replacement (Figure 6A). A common feature of the mutants was that cells tended to become multinucleate. The most striking effect was observed in the double

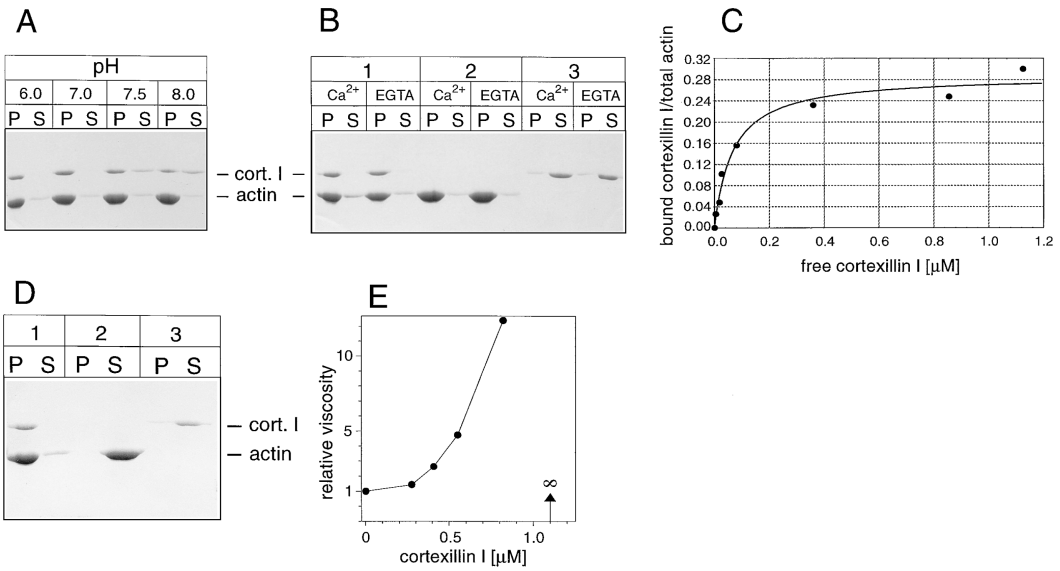

Figure 4. Cortexillin I Binding to F-Actin

(A) pH dependence of the cosedimentation of cortexillin I with F-actin showing an optimum between pH 6.0 and 7.0. Cortexillin I (0.5 μM of dimers) was incubated with actin (5 μM of subunits) in standard polymerization buffer, and proteins recovered in the pellet (P) and the supernatant (S) after high speed centrifugation were stained with Coomassie blue.

(B) Ca^{2+} independence of binding. The proteins were fractionated in imidazole buffer (pH 7.0) in the presence of 200 μM Ca^{2+} or 1 mM EGTA. Other conditions were as in (A). Panel 1 is cortexillin I with F-actin; panel 2 is F-actin alone; panel 3 is cortexillin I only.

(C) Binding curve showing a maximal ratio of 1 cortexillin I dimer bound per 3–4 actin subunits. Cortexillin I was mixed with 2.5 μM actin in standard polymerization buffer (pH 7.0), and its cosedimentation was assessed by high speed centrifugation.

(D) Low speed centrifugation shows that after preincubation with cortexillin I (panel 1), most of the F-actin was associated with complexes that form a pellet under conditions where, without cortexillin I (panel 2), practically all the actin filaments remained in the supernatant. Cortexillin I alone showed only faint accumulation in the pellet (panel 3). Incubation and staining were as in (A).

(E) Low shear viscometry reveals that complexes of cortexillin I with actin filaments form a gel. The viscosity of F-actin at a subunit concentration of 12 μM increased sharply between 0.5 and 1.0 μM cortexillin I dimer, and at 1.1 μM the viscosity became unmeasurably high (∞).

knockout mutant, in which more than 50% of the nuclei resided in cells with more than 10 nuclei (Figure 6B). Sometimes more than 90 nuclei were found in a single cell. This dramatic increase in nuclear numbers was due to an impairment of cytokinesis. Mitosis occurring synchronously in the multiple nuclei of a giant cell was

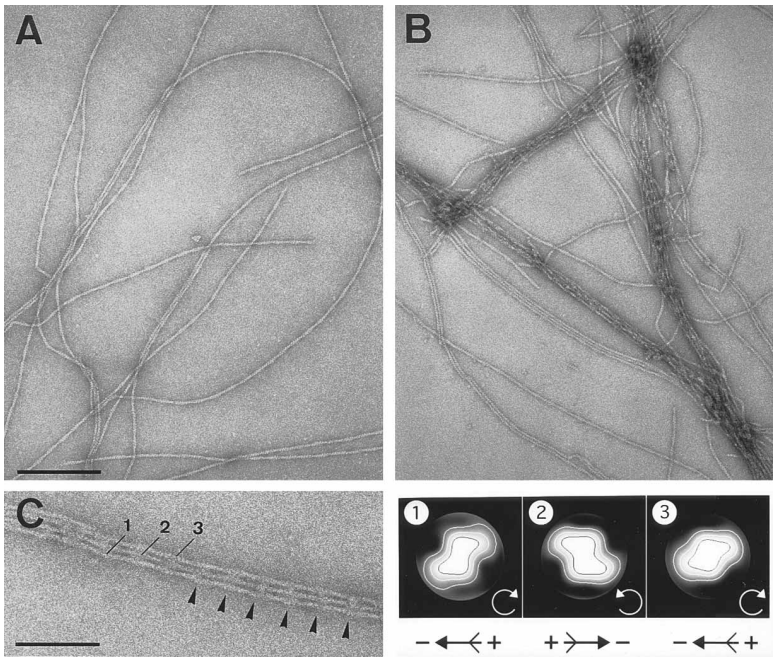

Figure 5. Arrangement of Actin Filaments Cross-Linked by Cortexillin I

(A) Dispersed filaments formed by pure rabbit muscle actin stabilized with phalloidin.

(B) Single-layered arrays, bundles, and meshworks of actin filaments produced by cortexillin I. Bar in (A) and (B) is 200 nm.

(C) Left, high magnification section of a single-layered, trimeric array of actin filaments (1 to 3) aligned by cortexillin I bridges (arrowheads). Bar is 100 nm. Right, relative polarities of the three filaments in the left panel, represented as axial projections of three-dimensional reconstructions. As indicated by the vorticities of the three projections, adjacent filaments had opposite polarities in this example. G-actin (5 μM) was incubated before polymerization with 0.25 μM cortexillin I dimer for (B) and with 0.18 μM cortexillin I dimer for (C).

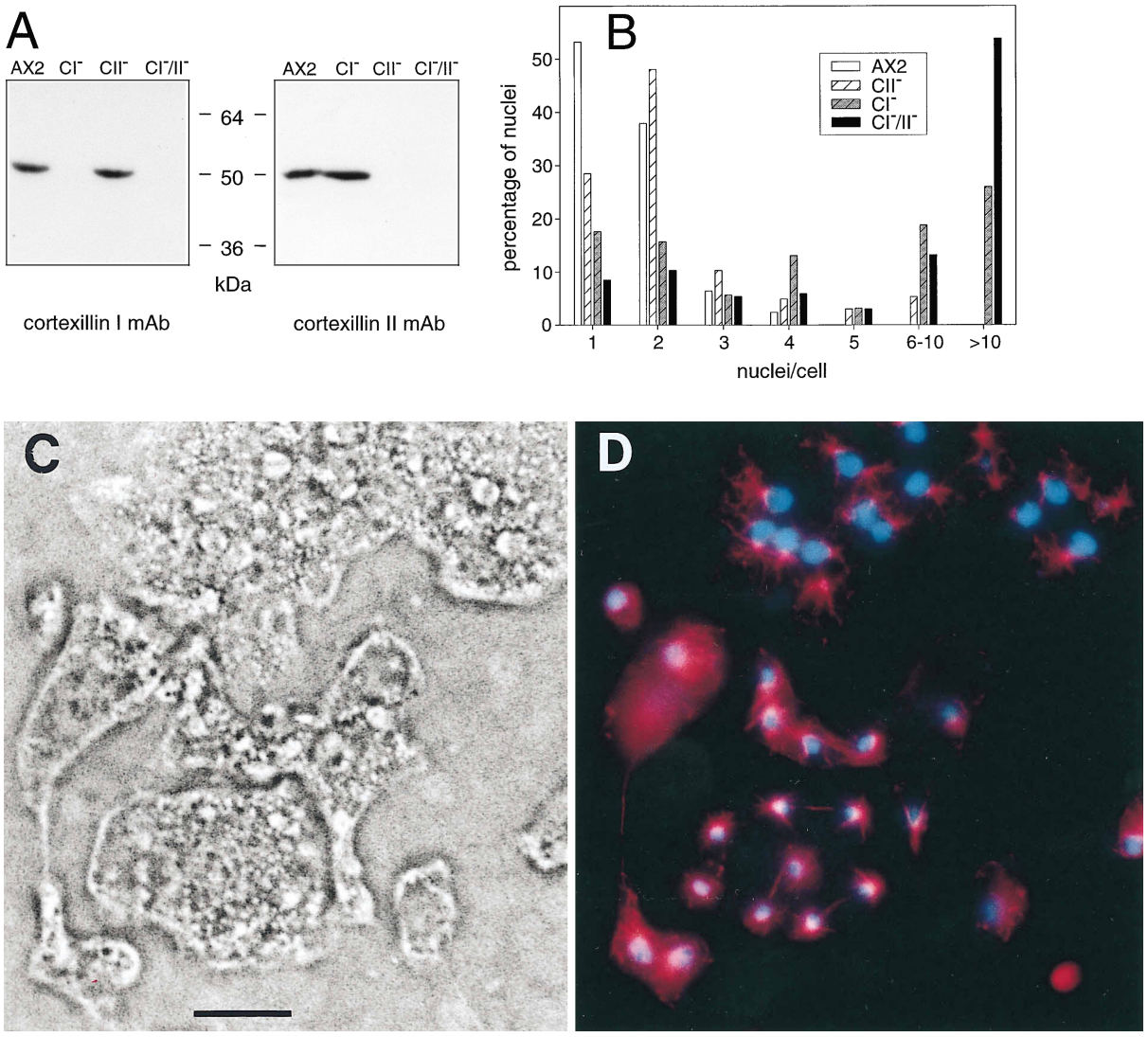

Figure 6. Increase in the Number of Nuclei per Cell in Gene Disruption Mutants Lacking Cortexillin I or II or Both Cortexillins

(A) Immunoblots demonstrating the presence or absence of cortexillins in mutant strains. AX2, wild-type; CI⁻, cortexillin I null mutant; CII⁻, cortexillin II null mutant; CI⁻/II⁻, cortexillin null double mutant. Total proteins corresponding to 2×10^5 growth-phase cells were loaded per lane, separated by SDS–PAGE, and labeled on blots with MAb 241-438-1 (left) or MAb 232-238-10 (right). For specificities of the antibodies see Figure 2A. Proteins transferred to the nitrocellulose filters were finally stained with Ponceau S to confirm uniformity of loading.

(B) Histogram illustrating the probability of nuclei residing in cells containing 1–10 or more nuclei. Wild-type AX2 and mutant cells cultivated for 2 days on glass coverslips in nutrient medium were fixed, and the nuclei were stained with diamidophenylindole (DAPI). Between 260 and 400 cells of each strain were counted.

(C) Phase-contrast image showing heterogeneity of cell sizes in fixed cortexillin I⁻/II⁻ double-mutant cells. The bar is 10 μm.

(D) Fluorescence image of the same cells as in (C) stained with DAPI for DNA (blue) and with antibody for α-tubulin (red). The large mitotic cell below the center is in the telophase stage without undergoing cytokinesis. Synchronous division of the nuclei is recognized by the thin spindle between the separated groups of chromosomes. The interphase nuclei in the other cells are larger (according to Weijer et al. [1984], S phase immediately succeeds mitosis in D. discoideum), and the systems of microtubuli originating from the centrosomes show little overlap (large cell on top). In the bipartite cell on the left, microtubules are seen to penetrate the stretch of cytoplasm connecting the two poles of the cell.

not accompanied by cytoplasmic cleavage (Figures 6C and 6D).

In the scanning electron microscope, wild-type cells appeared to be of domed shape and quite uniform in size, interspersed only with a few flat cells (Figure 7A). Cells lacking cortexillin I appeared in general slightly larger and more flat than cells lacking cortexillin II, in accord with the number of nuclei in these cells (compare Figure 6B with Figures 7B and 7C). In both mutants carrying single cortexillin defects, phenotypic changes were much less obvious than in double mutants. An extensive flattening was observed in cells lacking both cortexillins (Figures 7D and 7E). When spread on a glass or plastic surface, these double-mutant cells were distinguished by rugged borders. Cell bodies were often divided into pieces, connected only by threads of cytoplasm (Figure 7D). Video recordings revealed that the threads could be repeatedly stretched and shortened

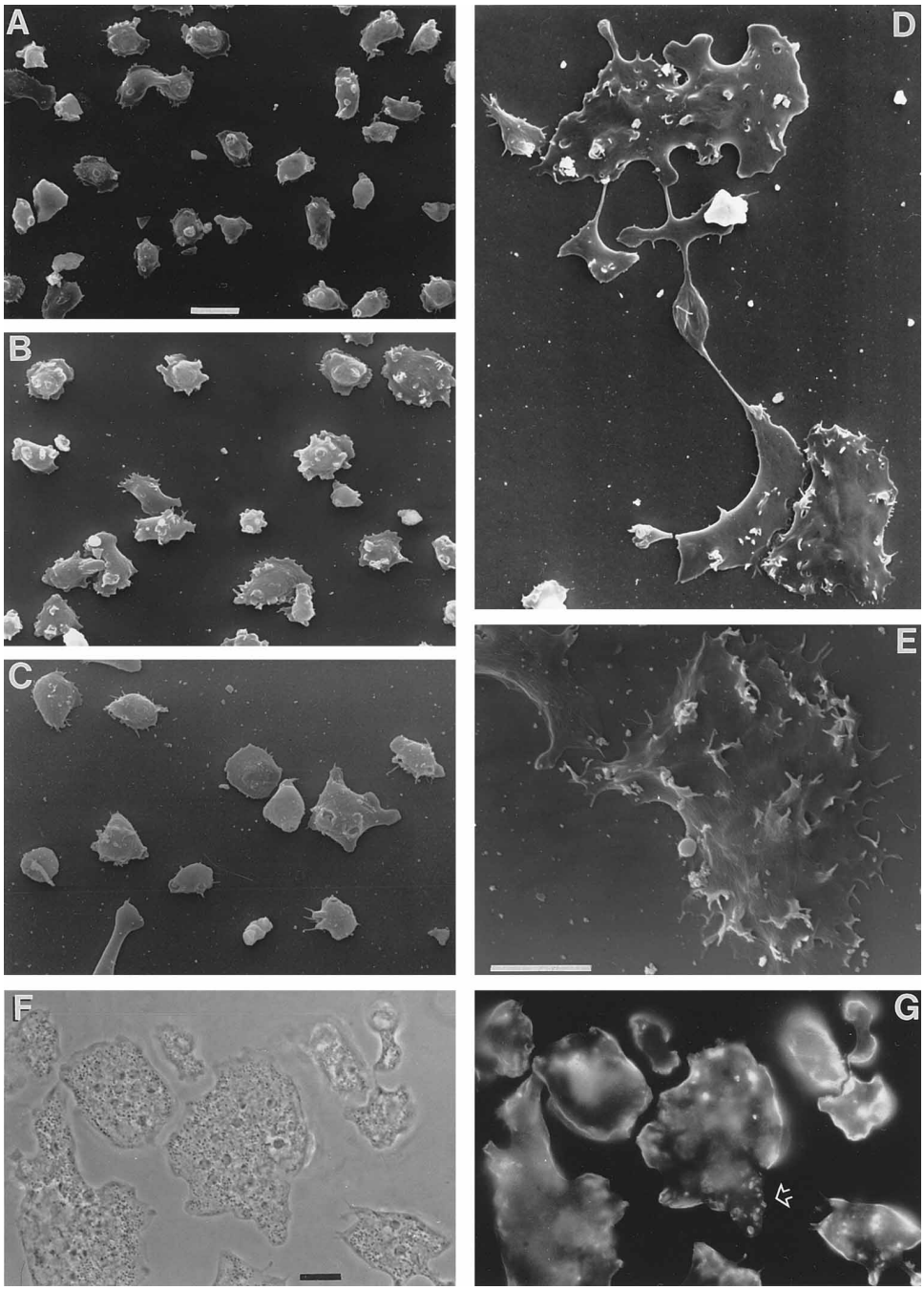

Figure 7. Shape and Size of Wild-Type and Cortexillin Mutant Cells and F-Actin Distribution in Cells Lacking Cortexillins I and II

(A–E) Scanning electron micrographs of cells from wild-type AX2 (A), cortexillin II null mutant (B), cortexillin I null mutant (C), and cortexillin I/II null double mutant (D and E). In (D), portions of a large cell are connected through thin cytoplasmic bridges. In the lower right corner a medium-sized cell is seen, and in the upper left edge a small cell of the double mutant is seen. The high magnification image in (E) of a flat double-mutant cell shows filopods at its border and tipped extensions of various shapes on its surface.

(F and G) Phase-contrast and fluorescence images of fixed double-mutant cells labeled with TRITC-conjugated phalloidin. The arrow in (G) indicates cell surface extensions, similar to the finger-like protrusions depicted in (E), at which F-actin is accumulated.

The cells had been cultivated for 2 days on glass coverslips in nutrient medium. The bars indicate 10 μm; magnification is the same in (A)–(D).

when portions of a cell moved in different directions. Sometimes the threads broke, giving rise to separate cells of variable size with an irregular number of nuclei. Despite their extreme flattening on a glass surface, the double-mutant cells had the capacity to cringe and even to detach transiently from the substrate.

The double-mutant cells formed filopods and crown-shaped extensions on their surfaces, similar to wild-type cells (Figure 7E). Phalloidin labeling indicated that F-actin accumulates in these extensions and forms a cortical layer, delineating the borders of the double-mutant cells (Figures 7F and 7G).

Since the inhibition of cytokinesis in cortexillin double mutants and the separation of pieces of the giant cells by traction-mediated cytofission were reminiscent of myosin II null mutant cells (Knecht and Loomis, 1987; DeLozanne and Spudich, 1987), we compared both mutants in cultures of cells attached to plastic petri dishes. The cortexillin I/II null cells were clearly distinguishable by their extreme flatness and size from the more compact and smaller cells of the myosin II mutant.

Discussion

Domain Organization of Cortexillin I

Four different regions can be distinguished in the cortexillin I molecules based on the sequence of their subunits and their architecture as revealed by TEM: the consensus actin-binding domain; a tail formed by a parallel two-stranded coiled coil; a region of less defined secondary structure; and a positively charged C-terminal nonapeptide.

The actin-binding domain is recognizable in the sequence as an N-terminal stretch of amino acids ending with His-226 (Figures 1C and 1D) and in the electron microscope as a globular head of 4–6 nm diameter (Figure 3A). With its two equivalent heads in juxtaposition, the dimeric molecule is capable of bundling actin filaments (Figure 5C). Flexible attachment of the heads to the tail of the molecule is proposed to be responsible for bundling the filaments in anti-parallel or, less often, parallel orientation.

By analytical ultracentrifugation, cortexillin I has been identified as a dimer. The heptad repeats $(a, b, c, d, e, f, g)_{18}$ between Ala-227 and Arg-352 correspond to a dimeric coiled coil with a calculated length of 19 nm (Figure 3F), in accord with a rod length measured by electron microscopy (Figure 3C). The sequence of this domain is consistent with a canonical coiled coil (McLachlan and Stewart, 1975; Cohen and Parry, 1990, 1994), in that hydrophobic residues prevail in the a and d positions of its 18 heptad repeats. Seven of the a positions are, however, occupied by positively charged residues. This is in contrast with the d positions, where only one repeat has a positively charged amino acid and two repeats have negatively charged residues (Figure 3F). The asymmetry between a and d positions is in accord with the coiled-coil structure of the leucine zipper in crystallized Fos-Jun transcription factor (Glover and Harrison, 1995).

The oligomerization properties of coiled-coil sequences are often determined by the distribution of β-branched residues in the a or d positions (Harbury et al., 1993, 1994). Valine and isoleucine in a favor dimerization, in d they favor tetramerization, and their presence in both a and d facilitates the formation of trimers. In the coiled-coil sequence of cortexillin I, neither valine nor isoleucine is present in the a or d positions, with the exception of one isoleucine in a of the last repeat. In addition to branched residues in a or d, charged residues are relevant to stoichiometry, stability, and orientation of coiled-coil domains. These residues are frequently found in positions e and g (Krylov et al., 1994; Zhou et al., 1994a, 1994b; Monera et al., 1994). In cortexillin I, negatively charged residues are particularly enriched in the e positions: 9 of the 18 repeats contain glutamic acid in this position.

The continuous 18 heptad repeat sequence in cortexillin I is followed by a 44 amino acid sequence of a less defined secondary structure including one proline and five glycine residues, which are unfavorable for α helix formation. Following this stretch, the COILS algorithm of Lupas et al. (1991) predicts a probability of 0.8 for a coiled-coil conformation (Figure 3E). If one assumes the sequence from Gly-405 to Ala-434 to be part of the rod domain, it would extend the length of the rod by 5 nm, which is at variance with the measured total rod length of 19 nm. The 2–3 nm globular domain in the C-terminal region observed by electron microscopy in about 30% of the cortexillin I molecules (Figures 3A and 3D) indicates that a segment of the sequence close to the C-terminus is capable of folding into a separate domain.

The positively charged sequence of the last nine C-terminal amino acid residues Lys-436 to Lys-444 is related to a consensus sequence for PIP_2 binding (Janmey et al., 1992; Hofmann, 1994), which has been found in gelsolin (Janmey and Stossel, 1987), gCap 39 (Yu et al., 1990), intestinal villin (Bazari et al., 1988), and Dictyostelium protovillin (Hofmann et al., 1993). Three residues in this nonapeptide of cortexillin I are serines flanked by lysines, which might be targets of protein kinase C, cyclic GMP–dependent protein kinase, or both (Pearson and Kemp, 1991).

The Growing α-Actinin/Spectrin Superfamily

Members of the α-actinin/spectrin superfamily are defined by common F-actin-binding motifs and are distinguished from each other by their rod and regulatory domains (De Arruda et al., 1990; Hartwig and Kwiatkowski, 1991; Matsudaira, 1991). According to the structure of these domains, the members can now be classified into the following four subfamilies.

First, fimbrins (plastins) are the only members that have two actin-binding sites in a single subunit and are thus as monomers capable of bundling actin filaments (Bretscher and Weber, 1980; De Arruda et al., 1990). The actin-binding sites in the fimbrin/plastin sequences are preceded by two EF hands, which make the binding of actin sensitive to Ca^{2+} (Pacaud and Harricane, 1987).

Second, triple α-helical repeat segments are common to the rods of α-actinin, spectrin, and dystrophin (Yan et al., 1993), and all three proteins contain complete or degenerated EF hands (Witke et al., 1993). In the spectrin tetramer, the EF hands and the actin-binding sites are located on different polypeptides, the α and β subunits. In dystrophin, the extremely long α-helical rod domain is extended not only by EF hands, but also by a coiled-coil region thought to be involved in the interaction with other proteins of the dystroglycan complex (Blake et al., 1995).

Third, like α-actinin, the 120 kDa gelation factor (ABP-120) of D. discoideum forms homodimers, which owe their F-actin cross-linking activity to the anti-parallel orientation of their subunits (Brink et al., 1990). The rod domain of ABP-120 is, however, made of cross–β sheet segments and resembles filamin in this respect. The

subunits of filamin are linked to each other at their C-terminal regions, so that the actin-binding domains are spread apart from each other at a wide angle (Gorlin et al., 1990; Matsudaira, 1991).

Fourth, the molecular architecture of cortexillin is unique among the members of the α-actinin/spectrin superfamily. Via their tail domains, two subunits are combined in parallel by forming a two-stranded α-helical coiled coil, thereby giving rise to a molecule that, with its two actin-binding heads, has the appearance in electron micrographs of a small double-headed myosin molecule.

Role of Cortexillins in Stabilizing Cell Shape and Enabling Cells to Divide

The elimination of cortexillins I and II by gene disruption interfered with cytokinesis. As a result, giant cells containing numerous nuclei emerged, similar but not identical to those obtained by eliminating myosin II in Dictyostelium cells (DeLozanne and Spudich, 1987; Knecht and Loomis, 1987). These similarities suggest that cortexillins can act in a complex together with actin and myosin in linking cytokinesis to nuclear division. The differences, primarily the extreme flatness of cortexillin I/II null cells, indicate that the cortexillins also have activities that are independent of myosin II.

With their two actin-binding heads orientated in the same direction, cortexillins are optimally designed to gather actin filaments together into meshworks of bundles. It is easy to imagine that the lack of these proteins destabilizes the cells to an extent that they collapse onto a substratum like a fried egg, even though actin filaments are still in the cortex. Although the general appearance of double-mutant cells justifies this notion, several observations indicate that this view is too simple. First, the double-mutant cells can transiently contract and then assume a more vaulted shape. Second, even when they are flat, these cells generate surface structures similar to the protrusions seen on the surface of wild-type cells. Actin filaments are accumulated in these protrusions and also at the border of the flat cell bodies. Evidently, the absence of cortexillins does not cause the actin filaments to remain dispersed in the cytoplasm. They can be assembled and connected with the plasma membrane.

The shape changes and surface extensions in the double-mutant cells are most likely supported by actin-cross-linking proteins still present in these cells. The cortexillin mutants may help to specify the function of these proteins in vivo. There are five other cross-linking proteins known from D. discoideum cells, of which three, α-actinin, ABP-120, and plastin (Prassler, 1995), possess actin-binding sites of the α-actinin/spectrin type (for review see Schleicher and Noegel, 1992). Elimination of any one of these three proteins failed to alter cell shape, size, or behavior severely (Brink et al., 1990; Cox et al., 1992; Wallraff et al., 1986; Prassler, 1995). Only when the two F-actin-cross-linking proteins, α-actinin and ABP-120, were eliminated together was development at the multicellular stage (under certain conditions) strongly affected, indicating that the presence of one of these proteins can partially compensate for loss of the other (Witke et al., 1992).

The cortexillins provide another example of a pair of proteins that need to be eliminated together for a dramatic phenotypic alteration to occur. The slight alterations found in mutants lacking only one isoform were somewhat more pronounced in cortexillin I–deficient cells than in cortexillin II–deficient cells (Figures 6B, 7B, and 7C). Further investigation utilizing directed mutagenesis will determine whether or not the C-terminal cluster of positively charged amino acids in cortexillin I (Figure 1B) is responsible for the primary importance of this isoform in cytokinesis.

Elimination of the two cortexillins demonstrated a stronger impact on cell shape than elimination of the other F-actin-cross-linking proteins that have been previously knocked out in Dictyostelium, either alone or pairwise. We conclude that cortexillins fulfil a basic function in determining cell shape and facilitating cytokinesis. Other actin-cross-linking proteins appear to have more of a modulating or fine-tuning function in adapting the activities of the cells to variations in environmental conditions, and thus linking cell behavior to chemotactic and other stimuli (Schindl et al., 1995; Weber et al., 1995).

Experimental Procedures

Growth and Development of Dictyostelium Cells

D. discoideum wild-type strain AX2 was cultivated in liquid medium at 23°C in suspension shaken at 150 rpm (Claviez et al., 1982). For development to aggregation competence, cells were washed twice in 17 mM K-Na phosphate buffer (pH 6.0), resuspended at a density of 10^7 cells per milliliter in the buffer, and shaken as before for 7 hr. For comparison of wild type with mutants that lack cortexillins or myosin II (Manstein et al., 1989), cells were cultivated on glass coverslips in nutrient medium on the bottom of petri dishes.

Protein Purification

Actin was purified from rabbit skeletal muscle for binding assays as described by Rees and Young (1967) and for electron microscopy according to Bremer et al. (1994).

An actin–myosin complex was prepared from AX2 cell lysates according to Fechheimer and Taylor (1984). After 15 hr in the cold, a second precipitate, which contained actin together with the F-actin-binding proteins α-actinin and ABP-120, was obtained from the supernatant of the first precipitate via centrifugation at 10,000 × g. This precipitate was dialyzed against 25 mM Tris–HCl (pH 8.4), 1 mM DTT, 1 mM benzamidine. The dissolved proteins were fractionated on a DE52 column, eluted with a linear gradient of 0–1000 mM NaCl, dialyzed against 25 mM Tris–HCl, 100 mM NaCl, 1 mM DTT, 1 mM benzamidine, loaded on a Sepharose S300 column, subjected to FPLC on a Mono Q column (Pharmacia, Uppsala, Sweden) in a buffer containing 25 mM Tris–HCl (pH 8.4) and 1 mM DTT, and eluted in a linear NaCl gradient. Proteins in these fractions were analyzed by SDS–PAGE in 10% gels and Coomassie blue staining. A 50 kDa protein cofractionating with α-actinin turned out to be cortexillin I.

Protein and DNA Sequence Analysis

N-terminal sequences were obtained from cortexillin and from LysC fragments resolved by reversed-phase chromatography by Edman degradation on an Applied Biosystems gas phase sequencer according to Eckerskorn et al. (1988).

Degenerated oligonucleotides based on N-terminal and internal peptide sequences were employed to prime a PCR using genomic DNA of the AX2 strain as a template. The 0.6 kb probe generated was labeled with [α-^{32}P]dATP and employed to screen a λgt11 cDNA library (Clonetech Inc., Palo Alto, CA) at 50% formamide for cortexillin I cDNA clones. To isolate cortexillin II cDNA, the library was screened with the same probe at 30% formamide. Positive clones were rescreened with a 3′ probe of cortexillin I at 50% formamide.

One phage not labeled under these conditions carried the complete sequence of cortexillin II.

DNA double strands were sequenced using the dideoxy chain termination method in both directions. The sequences were analyzed using the UWGCG software (Devereux et al., 1984) and the MIPSX database (Max-Planck-Institut, Martinsried, Federal Republic of Germany). For coiled coil prediction, matrices MTK and MTIDK of the COILS version 2.1 algorithm (Lupas et al., 1991) were used with a window size of 21. Weighting options were applied and a probability curve was generated by Cricket graph.

Production of His-Tagged Cortexillin I in E. coli

A cDNA fragment coding for residues Gly-3 to Lys-444 of cortexillin I was obtained by PCR using primers designed to obtain a BamHI site at the 5′ end and a HindIII site at the 3′ end. The amplified product was cloned into expression vector pQE32 (QIAGEN, Chatsworth, CA), the sequence was verified, and the His-tagged cortexillin I was expressed in E. coli M15. The product was purified from the soluble fraction of bacterial extracts on Ni^{2+}–NTA–agarose (QIAGEN) and used for all studies on cortexillin I structure and function.

Monoclonal Antibodies and Immunofluorescence Labeling

Antibodies were obtained by immunizing BALB/c mice with N-terminally His-tagged cortexillin I or II purified from E. coli, using either Freund's or aluminium hydroxide as an adjuvant. Spleen cells were fused with $PAIB_3Ag8I$ myeloma cells. MAb 241-36-2 and MAb 241-438-1 specifically recognized cortexillin I; MAb 232-238-10 proved to be specific for cortexillin II, as tested by solid phase assays and by immunoblotting after SDS–PAGE. One antibody, MAb 232-470-5, recognized an epitope on the N-terminal fusion peptides of the pQE 30-32 His-tag expression vectors (QIAGEN). For immunoblots the antibodies were ^{125}I labeled by the chloramine-T method.

For Figure 2, cells from suspension cultures were allowed to adhere for 30 min on glass coverslips; for Figures 6 and 7 cells were cultivated for 2 days on coverslips in nutrient medium. The cells were fixed for 15 min in a solution of 15% saturated picric acid, 2% paraformaldehyde (pH 6.0) postfixed with 70% ethanol and processed according to Humbel and Biegelmann (1992). Cortexillins were labeled with MAbs and TRITC-conjugated goat anti–mouse IgG (Jackson ImmunoResearch Laboratories Inc., West Grove, PA), F-actin with TRITC-phalloidin (Sigma), and α-tubulin with rat MAb YL 1/2 (Kilmartin et al., 1982) and TRITC-conjugated goat anti-rat antibodies (Jackson ImmunoResearch). Micrographs were taken with a Phaco 100× oil Neofluar objective using a Zeiss Axiophot microscope.

Gene Replacement in D. discoideum

A cortexillin II–targeting vector was constructed by inserting of the Blasticidin (Bsr) cassette from plasmid pBsr2 (Sutoh, 1993) into the single blunted HindIII site of cortexillin II cDNA, which encodes the consensus actin-binding domain of cortexillin II. The construct was excised with EcoRI, and the linearized fragment was used for calcium phosphate–mediated transformation to disrupt the cortexillin II gene in the AX2 wild-type strain. Four independent cortexillin II null transformants were selected with 10 μg/ml Blasticidin S (ICN) in nutrient medium and identified by the colony blot technique (Wallraff and Gerisch, 1991) employing ^{125}I-labeled MAb 232-238-10.

For construction of a cortexillin I targeting vector, a 260 bp 5′ HindIII–EcoRI fragment and a 600 bp 3′ EcoRI–HindIII fragment of the cortexillin I gene were synthesized by PCR using the primers 5′-GCGAAGCTTACACAATACATATAAAAGATG-3′ and 5′-CGCGAATTCAAGGAATTTAAGAGCAAGTGC-3′ for the 5′ fragment, and 5′-CGCGAATTCATTGGAATCTGAAAAGGT-3′ and 5′-GCGAAGCTTTTTAATTTATTTTTTTGATTTTGATGAT-3′ for the 3′ fragment. After cleavage with HindIII and EcoRI, both fragments were gel purified and ligated with T4 DNA ligase. The ligase mixture was digested with HindIII, and the resulting 860 bp fragment was cloned into the HindIII sites of pIC20H. This plasmid was linearized with EcoRI, and the ends were blunted with Klenow fragment and ligated with a blunted 2.2 kb G418 resistance cassette from plasmid B10 (Nellen et al., 1984). The 3.1 kb fragment of cortexillin I cDNA containing the G418 cassette was excised with HindIII and used for disruption of the cortexillin I gene. Three independent cortexillin I null mutants were selected with 10 μg/ml G418 (Sigma) in nutrient medium from AX2 wild type and identified by colony blotting with ^{125}I-MAb 241-438-1. In the same way, six independent cortexillin I/II double mutants all producing large cells were obtained from cortexillin II null cells.

Analytical Methods

CD spectra of His-tagged cortexillin I were recorded in G buffer containing 2 mM Tris–HCl, 0.2 mM Na_2ATP, 0.5 mM DTT, 0.2 mM $CaCl_2$, and 0.01% NaN_3 (pH 7.2) at room temperature on a Dichrograph Mark IV from Jobin Yvon (Longjumeau, France), equipped with a thermostated cell holder and connected to a data station for signal averaging and processing. α Helix content was estimated on the basis of $\theta_{222} = 36{,}000$ deg cm^2 dmol^{-1} for 100% α helix, applying the rigid criterion of Finkelstein et al. (1977).

Analytical ultracentrifugation was performed on an Optima XLA analytical ultracentrifuge (Beckman Instruments, Palo Alto, CA) equipped with an absorption optical system (Terzi et al., 1994). The concentration of recombinant cortexillin I was adjusted to $OD_{276} = 0.1$, and the protein was analyzed at 20°C in 5 mM sodium phosphate buffer (pH 7.4) supplemented with 150 mM NaCl. Sedimentation velocity experiments were performed at 56,000 rpm in a 12 mm epon double-sector cell, which was filled with 0.12 ml of sample solution in one sector and the same volume of buffer measured at 230 nm in the other. Sedimentation coefficients were corrected to water by the standard procedure (Eason, 1986). Sedimentation equilibrium runs were performed at 12,000 rpm. An average molecular mass was determined using linear regression analysis to obtain the best linear fit of ln A versus r^2 plots. A partial specific volume of 0.73 ml/g was used for the calculations, deduced from the amino acid composition of cortexillin I.

Low or high stringency Southern blots were hybridized for 15 hr at 37°C in 2× SSC (standard salt citrate) containing 30% or 50% formamide. SDS–PAGE followed standard procedures. The concentration of G-actin was determined at 290 nm using an absorption coefficient of 24,900 M^{-1} cm^{-1} (Wegner, 1976). The concentration of cortexillin I was determined according to Bradford (1976) and calibrated by total amino acid analysis on a Beckman 6300 amino acid analyzer.

Electron Microscopy

For scanning electron microscopy, cells were cultivated for 2 days on 12 mm glass coverslips with nutrient medium in a petri dish at 23°C and were immediately fixed after removal of excess medium according to Claviez et al. (1986) with 1% glutaraldehyde and 0.02% osmium tetroxide. Critical point dried specimens were gold coated to 20 nm with a Balzers SCD 020 Coating Unit (Balzers, Liechtenstein) and examined with a JEOL JSM 35C scanning electron microscope at 25 kV.

For glycerol spraying/low angle rotary metal shadowing of cortexillin I molecules, 20 μl of recombinant His-tagged cortexillin I, 0.1–0.3 mg/ml in 5 mM Na-phosphate, 150 mM NaCl (pH 7.4), plus 30% glycerol, were sprayed with or without 0.1–0.3 mg/ml MAb 232-470-5 onto freshly cleaved mica and rotary shadowed in a BA 511 M freeze-etch apparatus (Balzers) with platinum–carbon at an elevation angle of 3°–5° (Fowler and Aebi, 1983). Molecular rod length distributions measured on micrographs were fitted by single Gaussian curves using the Marquaradt algorithm.

F-actin bundles were obtained from mixtures of G-actin with His-tagged cortexillin I within 1 hr after the addition of 2 mM $MgCl_2$, 50 mM KCl and stoichiometric amounts of phalloidin relative to actin (Bremer et al., 1994). Samples (5 μl) were adsorbed for 1 min to a glow-discharged (Aebi and Pollard, 1987) carbon-coated collodion film on a copper grid. The grid was then washed on two drops of distilled water before it was sequentially placed on two drops of 0.75% uranyl formate (pH 4.25), for a total of about 15 s. Electron micrographs were taken in a Hitachi H-7000 TEM operated at 100 kV on Kodak SO-163 electron image film at 50,000× nominal magnification, calibrated according to Wrigley (1968). The polarity of actin filaments was determined according to Bremer et al. (1994). A filament pair revealing axial projections with the same vorticity meant that the two filaments had the same polarity, whereas axial projections with opposite vorticities meant that the two adjacent filaments had opposite polarities (Meyer and Aebi, 1990).

F-Actin Binding and Cross-Linking Assays

Low shear viscometry was carried out at 20°C in a falling ball viscometer (MacLean-Fletcher and Pollard, 1980) in 2 mM $MgCl_2$, 10 mM imidazole (pH 7.0), 1 mM ATP, 0.2 mM $CaCl_2$. Viscosity was determined at 30 min after the addition of 80 μg of G-actin per 160 μl of incubation mixture.

For high speed sedimentation assays, G-actin and cortexillin I solutions were cleared for 30 min in the cold at 27 psi in a Beckman airfuge, and the reaction mixtures were incubated for 2 hr at room temperature in Beckman Ultra-Clear centrifugation tubes in standard polymerization buffer (10 mM MOPS containing 2 mM $MgCl_2$ and 50 mM KCl) at the pH values indicated or in imidazole buffer (10 mM imidazole containing 3 mM $MgCl_2$, 1 mM ATP, and either 0.2 mM $CaCl_2$ or 1 mM EGTA [pH 7.0]). Samples (160 μl) were centrifuged as above in the airfuge, and the pellets were brought to the original volume in SDS sample buffer. To quantitate cosedimentation of cortexillin I with actin, proteins were blotted after SDS–PAGE onto nitrocellulose, incubated with MAb 232-470-5, and labeled with sheep [^{125}I]anti–mouse IgG. Calculation of free and bound cortexillin I was based on determining the ratio of radioactivity in the 50 kDa band from the pellet and supernatant fractions with a Fuji Phosphoimager. An average K_D value was calculated from the data of Figure 4C, omitting the three points obtained at high cortexillin I concentrations.

For low speed sedimentation, the proteins were incubated for 2 hr at room temperature in standard polymerization buffer (pH 7.0) sedimented for 30 min at 16,000 × g in an Eppendorf centrifuge, and analyzed in supernatant and pellet fractions as described.

Acknowledgments

Correspondence should be addressed to J. F. We thank Ariel Lustig (Biozentrum der Universität Basel) for performing the analytical ultracentrifugation experiments, Dr. Luis Moroder and Daniela Quarzago for CD measurements, and Uta Shimanko (Max-Planck-Institut für Biochemie) for the synthesis of oligonucleotides and Angelika Konzok and Christina Heizer for assistance. We are grateful to Drs. Chris Clougherty and Gerard Marriott for critical reading of the manuscript. This work was supported by the Max-Planck-Gesellschaft and the Swiss National Science Foundation (31-39691.93), the Stipendienfonds der Basler Chemischen Industrie, the Department of Education of the Kanton Basel–Stadt, and the M. E. Müller Foundation of Switzerland.

Received January 8, 1996; revised July 5, 1996.

References

Aebi, U., and Pollard, T.D. (1987). A glow discharge unit to render electron microscope grids and other surfaces hydrophilic. J. Electron Microsc. Tech. *7*, 29–33.

Bazari, W.L., Matsudaira, P., Wallek, M., Smeal, T., Jakes, R., and Ahmed, Y. (1988). Villin sequence and peptide map identify six homologous domains. Proc. Natl. Acad. Sci. USA *85*, 4986–4990.

Blake, D.J., Tinsley, J.M., Davies, K.E., Knight, A.E., Winder, S.J., and Kendrick-Jones, J. (1995). Coiled-coil regions in the carboxy-terminal domains of dystrophin and related proteins: potentials for protein-protein interactions. Trends Biochem. Sci. *20*, 133–135.

Bradford, M.M. (1976). A rapid and sensitive method for quantification of microgram quantities of protein utilizing the principle of protein dye-binding. Anal. Biochem. *72*, 248–254.

Bremer, A., Henn, C., Goldie, K.N., Engel, A., Smith, P.R., and Aebi, U. (1994). Towards atomic interpretation of F-actin filament three-dimensional reconstruction. J. Mol. Biol. *242*, 683–700.

Bretscher, A., and Weber, K. (1980). Fimbrin, a new microfilament-associated protein present in microvilli and other cell surface structures. J. Cell Biol. *86*, 335–340.

Brink, M., Gerisch, G., Isenberg, G., Noegel, A.A., Segall, J.E., Wallraff, E., and Schleicher, M. (1990). A *Dictyostelium* mutant lacking an F-actin cross-linking protein, the 120 kD gelation factor. J. Cell Biol. *111*, 1477–1489.

Claviez, M., Pagh, K., Maruta, H., Baltes, W., Fisher, P., and Gerisch, G. (1982). Electron microscopic mapping of monoclonal antibodies on the tail region of *Dictyostelium* myosin. EMBO J. *1*, 1017–1022.

Claviez, M., Brink, M., and Gerisch, G. (1986). Cytoskeletons from a mutant of *Dictyostelium discoideum* with flattened cells. J. Cell Sci. *86*, 69–82.

Cohen, C., and Parry, D.A.D. (1990). α-Helical coiled-coils: how to design an α-helical protein. Proteins *7*, 1–15.

Cohen, C., and Parry, D.A.D. (1994). α-Helical coiled-coils: more facts and better prediction. Science *265*, 488–489.

Cox, D., Condeelis, J., Wessels, D., Soll, D., Kern, H., and Knecht, D.A. (1992). Targeted disruption of the ABP-120 gene leads to cells with altered motility. J. Cell Biol. *116*, 943–955.

De Arruda, M.V., Watson, S., Lin, C.-S., Leavitt, J., and Matsudaira, P. (1990). Fimbrin is a homologue of the cytoplasmatic phosphoprotein plastin and has domains homologous with calmodulin and actin gelation proteins. J. Cell Biol. *111*, 1069–1079.

DeLozanne, A., and Spudich, J.A. (1987). Disruption of the *Dictyostelium* heavy chain gene by homologous recombination. Science *236*, 1086–1091.

Devereux, J., Haeberli, P., and Smithies, O. (1984). A comprehensive set of sequence analysis programs for the VAX. Nucl. Acids Res. *12*, 387–395.

Eason, R. (1986). Analytical ultracentrifugation. In Centrifugation, A Practical Approach, Second Edition, D. Rickwood, ed. (Oxford and Washington, D.C.: IRL Press), pp. 251–286.

Eckerskorn, C., Mewes, W., Goretzki, H., and Lottspeich, F. (1988). A new siliconized-glass fiber as support for protein-chemical analysis of electroblotted proteins. Eur. J. Biochem. *176*, 509–519.

Fechheimer, M., and Taylor, D.L. (1984). Isolation and characterization of a 30,000 dalton calcium sensitive actin cross-linking protein from *Dictyostelium discoideum*. J. Biol. Chem. *259*, 4514–4520.

Finkelstein, A.V., Ptitsyn, O.B., and Kozitsyn, S.A. (1977). Theory of protein molecule self-organization. II. A comparison of calculated thermodynamic parameters of local secondary structures with experiments. Biopolymers *16*, 497–524.

Fowler, W.E., and Aebi, U. (1983). Preparations of single molecules and supramolecular complexes for high-resolution metal shadowing. J. Ultrastruct. Res. *83*, 319–334.

George, E.L., Ober, M.B., and Emerson, C.P., Jr. (1989). Functional domains of the *Drosophila melanogaster* muscle myosin heavy-chain gene are encoded by alternatively spliced exons. Mol. Cell. Biol. *9*, 2957–2974.

Glover, J.N.M., and Harrison, S.C. (1995). Crystal structure of the heterodimeric bZIP transcription factor c-Fos-c-Jun bound to DNA. Nature *373*, 257–261.

Gorlin, J.B., Yamin, R., Egan, S., Stewart, M., Stossel, T.P., Kwiatkowski, D.J., and Hartwig, J.H. (1990). Human endothelial actin-binding protein (ABP-280, non-muscle filamin): a molecular leaf spring. J. Cell Biol. *111*, 1089–1105.

Harbury, P.B., Zhang, T., Kim, P.S., and Alber, T. (1993). A switch between two, three and four stranded coiled-coils in GCN4 leucine zipper mutants. Science *262*, 1401–1407.

Harbury, P.B., Kim, P.S., and Alber, T. (1994). Crystal structure of an isoleucine-zipper trimer. Nature *371*, 80–83.

Hartwig, J.H., and Kwiatkowski, D.J. (1991). Actin-binding proteins. Curr. Opin. Cell Biol. *3*, 87–97.

Hofmann, A. (1994). Isolierung und Charakterisierung von Protovillin, einem neuartigen F-Aktin verkappenden Protein aus *Dictyostelium discoideum*. PhD thesis, University of Bayreuth, Bayreuth, Federal Republic of Germany.

Hofmann, A., Noegel, A.A., Bomblies, L., Lottspeich, F., and Schleicher, M. (1993). The 100 kDa F-actin capping protein of *Dictyostelium* amoebae is a villin prototype ("protovillin"). FEBS Lett. *328*, 71–76.

Hu, R.J., Watanabe, M., and Bennett, V. (1992). Characterization of human brain cDNA encoding the general isoform of β-spectrin. J. Biol. Chem. *267*, 18715–18722.

Humbel, B.M., and Biegelmann, E. (1992). A preparation protocol for postembedding immunoelectron microscopy of *Dictyostelium discoideum* with monoclonal antibodies. Scanning Microsc. *6*, 817–825.

Janmey, P.A., and Stossel, T.P. (1987). Modulation of gelsolin function by phosphatidylinositol 4,5-bisphosphate. Nature *325*, 362–364.

Janmey, P.A., Lamb, J., Allen, P.G., and Matsudaira, P.T. (1992). Phosphoinositide-binding peptides derived from the sequences of gelsolin and villin. J. Biol. Chem. *267*, 11818–11823.

Kilmartin, J.V., Wright, B., and Milstein, C. (1982). Rat monoclonal antibodies derived by using a new nonsecreting rat cell line. J. Cell Biol. *93*, 576–582.

Knecht, D.A., and Loomis, W.F. (1987). Antisense RNA inactivation of myosin heavy chain expression in *Dictyostelium discoideum*. Science *236*, 1081–1086.

Krylov, D., Mikhailenko, I., and Vinson, C. (1994). A thermodynamic scale for leucine zipper stability and dimerization specificity: e and g interhelical interactions. EMBO J. *13*, 2849–2861.

Luna, E.J., and Condeelis, J.S. (1990). Actin-associated proteins in *Dictyostelium discoideum*. Dev. Genet. *11*, 328–332.

Lupas, A., Van Dyke, M., and Stock, J. (1991). Predicting coiled coils from protein sequences. Science *252*, 1162–1164.

MacLean-Fletcher, S.D., and Pollard, T.D. (1980). Viscometric analysis of the gelation of *Acanthamoeba* extracts and purification of two gelation factors. J. Cell Biol. *85*, 414–428.

Manstein, D.J., Titus, M.A., DeLozanne, A., and Spudich, J.A. (1989). Gene replacement in *Dictyostelium*: generation of myosin null mutants. EMBO J. *8*, 923–932.

Matsudaira, P. (1991). Modular organization of actin crosslinking proteins. Trends Biochem. Sci. *16*, 87–92.

McLachlan, A.D., and Stewart, M. (1975). Tropomyosin coiled-coil interactions: evidence for an unstaggered structure. J. Mol. Biol. *98*, 293–304.

Meyer, R.K., and Aebi, U. (1990). Bundling of actin filaments by α-actinin depends on its molecular length. J. Cell Biol. *110*, 2013–2024.

Monera, O.D., Khy, C., and Hodges, R.S. (1994). Electrostatic interactions control the parallel and antiparallel orientation of α-helical chains in two stranded α-helical coiled-coil. Biochemistry *33*, 3862–3872.

Nellen, W., Silan, C., and Firtel, R.A. (1984). DNA-mediated transformation of *Dictyostelium discoideum*: regulated expression of an actin gene fusion. Mol. Cell. Biol. *4*, 2890–2898.

Pacaud, M., and Harricane, M.C. (1987). Calcium control of macrophage cytoplasmic gelation: evidence for the involvement of the 70,000 M_r actin-bundling protein. J. Cell Sci. *88*, 81–94.

Pearson, R.B., and Kemp, B.E. (1991). Protein kinase phosphorylation site sequences and consensus specificity motifs: tabulations. Meth. Enzymol. *200*, 62–81.

Pollard, T.D., and Cooper, J.A. (1986). Actin and actin-binding proteins: a critical evaluation of mechanisms and functions. Annu. Rev. Biochem. *55*, 987–1035.

Prassler, J. (1995). Plastin aus *Dictyostelium discoideum*: Isolierung, biochemische Charakterisierung und Ausschalten dieses aktinbindenden Proteins durch Geninaktivierung. PhD thesis, Technical University München, München, Federal Republic of Germany.

Raymond-Denise, A., Sansonetti, P.J., and Guillen, N. (1993). Isolation and characterization of a myosin heavy chain gene (mhcA) from the human parasitic pathogen *Entamoeba histolytica*. Mol. Biochem. Parasitol. *59*, 123–131.

Rees, M.K., and Young, M. (1967). Studies on the isolation and molecular properties of homogeneous globular actin: evidence for a single polypeptide chain. J. Biol. Chem. *242*, 4449–4458.

Schindl, M., Wallraff, E., Deubzer, B., Witke, W., Gerisch, G., and Sackmann, E. (1995). Cell-substrate interactions and locomotion of *Dictyostelium* wild-type and mutants defective in three cytoskeletal proteins: a study using quantitative reflection interference contrast microscopy. Biophys. J. *68*, 1177–1190.

Schleicher, M., and Noegel, A.A. (1992). Dynamics of the *Dictyostelium* cytoskeleton during chemotaxis. New Biol. *4*, 461–472.

St-Pierre, B., Couture, C., Laroche, A., and Pallotta, D. (1993). Two developmentally regulated mRNAs encoding actin-binding proteins in *Physarum polycephalum*. Biochim. Biophys. Acta *1173*, 107–110.

Sutoh, K. (1993). A transformation vector for *Dictyostelium discoideum* with a new selectable marker, bsr. Plasmid *30*, 150–154.

Terzi, E., Hölzemann, G., and Seelig, J. (1994). Reversible random coil β-sheet transitions of the Alzheimer β-amyloid fragment (25–35). Biochemistry *33*, 1345–1350.

Wallraff, E., and Gerisch, G. (1991). Screening of *Dictyostelium* mutants defective in cytoskeletal proteins by colony immunoblotting. Meth. Enzymol. *196*, 334–348.

Wallraff, E., Schleicher, M., Modersitzki, M., Rieger, D., Isenberg, G., and Gerisch, G. (1986). Selection of *Dictyostelium* mutants defective in cytoskeletal proteins: use of an antibody that binds to the ends of α-actinin rods. EMBO J. *5*, 61–67.

Weber, I., Wallraff, E., Albrecht, R., and Gerisch, G. (1995). Motility and substratum adhesion of *Dictyostelium* wild-type and cytoskeletal mutant cells: a study by RICM/bright-field double-view image analysis. J. Cell Sci. *108*, 1519–1530.

Wegner, A. (1976). Head to tail polymerisation of actin. J. Mol. Biol. *108*, 139–150.

Weijer, C.J., Duschl, G., and David, C.N. (1984). A revision of the *Dictyostelium discoideum* cell cycle. J. Cell Sci. *70*, 111–131.

Witke, W., Schleicher, M., and Noegel, A.A. (1992). Redundancy in the microfilament system: abnormal development of Dictyostelium cells lacking two F-actin cross-linking proteins. Cell *68*, 53–62.

Witke, W., Hofmann, A., Köppel, B., Schleicher, M., and Noegel, A.A. (1993). The Ca^{2+}-binding domains in non-muscle type α-actinin: biochemical and genetic analysis. J. Cell Biol. *121*, 599–606.

Wrigley, N.G. (1968). The lattice spacing of crystalline catalase as an internal standard of length in electron microscopy. J. Ultrastruct. Res. *24*, 454–464.

Yan, Y., Winograd, E., Viel, A., Cronin, T., Harrison, S.C., and Branton, D. (1993). Crystal structure of the repetitive segments of spectrin. Science *262*, 2027–2030.

Youssoufian, H., McAfee, M., and Kwiatkowski, D.J. (1990). Cloning and chromosomal localization of human cytoskeletal α-actinin gene reveals linkage to the β-spectrin gene. Am. J. Hum. Genet. *47*, 62–71.

Yu, F.-X., Johnston, P.A., Suedhof, T.C., and Yin, H.L. (1990). gCap39, a calcium ion- and polyphosphoinositide-regulated actin capping protein. Science *250*, 1413–1415.

Zhou, N.E., Khy, C., and Hodges, R.S. (1994a). The net energetic contribution of interhelical electrostatic attractions to coiled-coil stability. Protein Eng. *7*, 1365–1372.

Zhou, N.E., Khy, C., and Hodges, R.S. (1994b). The role of interhelical ionic interactions in controlling protein folding and stability: *de novo* designed synthetic two-stranded α-helical coiled-coils. J. Mol. Biol. *237*, 500–512.

GenBank Accession Numbers

The cDNA sequences described in this paper have been assigned GenBank accession numbers L49527 (cortexillin I) and L46371 (cortexillin II).